

1 Maramycin, a cytotoxic isoquinolinequinone terpenoid  
2 produced through heterologous expression of a bifunctional  
3 indole prenyltransferase /tryptophan indole-lyase in *S.*  
4 *albidoflavus*

5 Matiss Maleckis,<sup>1#</sup> Mario Wibowo,<sup>2,3#</sup> Sam E. Williams,<sup>1#</sup> Charlotte H. Gotfredsen,<sup>4</sup> Renata  
6 Sigrist,<sup>1</sup> Luciano D.O. Souza<sup>5,6</sup>, Michael S. Cowled,<sup>2</sup> Pep Charusanti,<sup>1</sup> Tetiana Gren,<sup>1</sup>  
7 Subhasish Saha,<sup>1</sup> José M. A. Moreira<sup>5</sup>, Tilmann Weber,<sup>1\*</sup> Ling Ding<sup>2\*</sup>

8 <sup>1</sup> The Novo Nordisk Foundation Center for Biosustainability, Technical University of Denmark, Søltofts Plads, Building 220, 2800 Kgs. Lyngby, Denmark.

10 <sup>2</sup> Department of Biotechnology and Biomedicine, Technical University of Denmark, Kongens Lyngby, Denmark, Søltofts Plads, Building 221, 2800 Kgs. Lyngby, Denmark

12 <sup>3</sup> Current address: Singapore Institute of Food and Biotechnology Innovation (SIFBI), Agency for Science, Technology and Research (A\*STAR), 138669, Singapore

14 <sup>4</sup> Department of Chemistry, Technical University of Denmark, Kongens Lyngby, Denmark

15 <sup>5</sup> Department of Drug Design and Pharmacology, Faculty of Health and Medical Sciences, University of Copenhagen, 2100 Copenhagen, Denmark;

17 <sup>6</sup> Sino-Danish Center for Education and Research (SDC), Aarhus University, 8000 Aarhus C, Denmark.

18

19 \*Correspondence can be addressed to Tilmann Weber ([tiwe@biosustain.dtu.dk](mailto:tiwe@biosustain.dtu.dk)) and Ling Ding ([lidi@dtu.dk](mailto:lidi@dtu.dk))

20 <sup>#</sup>Contributed equally

21

22 **Abstract**

23 Isoquinolinequinones represent an important family of natural alkaloids with profound  
24 biological activities. Heterologous expression of a rare bifunctional indole prenyltransferase  
25 /tryptophan indole-lyase enzyme from *Streptomyces mirabilis* P8-A2 in *S. albidoflavus* J1074  
26 led to the activation of a putative isoquinolinequinone biosynthetic gene cluster and production  
27 of a novel isoquinolinequinone alkaloid, named maramycin (**1**). The structure of maramycin  
28 was determined by analysis of spectroscopic (1D/2D NMR) and MS spectrometric data. The  
29 prevalence of this bifunctional biosynthetic enzyme was explored and found to be a recent  
30 evolutionary event with only a few representatives in Nature. Maramycin exhibited moderate  
31 cytotoxicity against human prostate cancer cell lines, LNCaP and C4-2B. The discovery of  
32 maramycin (**1**) enriched the chemical diversity of natural isoquinolinequinones and also  
33 provided new insights into crosstalk between the host biosynthetic genes and the heterologous  
34 biosynthetic genes in generating new chemical scaffolds.

35 **Introduction**

36 *Streptomyces* represent a prolific source for bioactive secondary metabolites, exemplified by  
37 the antibiotics streptomycin, tetracycline and daptomycin, and the anticancer drugs  
38 doxorubicin and bleomycin, all WHO essential medicines<sup>1</sup>.

39 The advances of modern genome mining analyses have revealed that still a large fraction of  
40 the biosynthetic potential is untapped: 70% of the secondary metabolites produced by  
41 *Streptomyces* are cryptic compounds whose corresponding genes are normally silent in  
42 standard laboratory culture conditions<sup>2–5</sup>. Many approaches, especially synthetic biology and  
43 ecology have been applied to access this genetic potential<sup>6,7</sup> by using, for example, genetic  
44 engineering<sup>8</sup>, heterologous expression of a BGC in another host<sup>9</sup>, chemical elicitors<sup>10</sup> and co-  
45 cultivation<sup>11</sup>. These strategies are often employed to unravel the potential of metabolite  
46 production of *Streptomyces* through cryptic gene activation, allowing for a vast number of  
47 potentially valuable compounds to be discovered.

48 Isoquinolinequinones represent an important family of natural alkaloids with profound  
49 biological activities. They are predominantly isolated from marine invertebrates, such as  
50 cytotoxic caulibugulones and perfragilins from the bryozoan *Caulibugula inermis*<sup>12</sup> and  
51 *Membranipora perfragilis*<sup>13</sup>, antineoplastic cibrostatins from the sponge *Cribrochalina* sp.<sup>14</sup>  
52 and antimicrobial and anti-inflammatory renierones from the sponge *Renier* sp.<sup>15</sup> and  
53 *Haliclona* sp.<sup>16</sup>. Hence, it was believed that isoquinolinequinones are natural products from  
54 marine invertebrates. However, the recent discovery of such compounds including the  
55 mansouramycins<sup>17–20</sup> and albumycin<sup>21</sup> from *Streptomyces* showed that microbes are also  
56 isoquinolinequinones producers. An isoquinolinequinone biosynthetic gene cluster in *S.*  
57 *albidoflavus* J1074 (previously recognized under the name *S. albus* J1074) was proposed by  
58 Chai et al.<sup>22</sup> where they identified three bicyclic isoquinolinequinone products when expressing  
59 a putative BGC in *S. coelicolor* M1146<sup>19</sup>. This BGC was further studied by Shuai et al.<sup>23</sup>, who

60 confirmed mansouramycin production in *S. albidoflavus* Del14<sup>24</sup>, a genome minimized strain  
61 of *S. albidoflavus* J1074<sup>25</sup>. Through feeding studies and NMR analysis, tryptophan was  
62 identified to be a precursor in the biosynthesis of mansouramycin D and tryptophan derived  
63 intermediates were detected in knockout strains<sup>23</sup>.

64

65 *S. albidoflavus* J1074 has been routinely used as a heterologous expression host system in our  
66 laboratory<sup>26-28</sup>. Although it harbors a putative mansouramycin BGC, we have not detected  
67 production of any related alkaloids under the laboratory conditions we routinely use. In a recent  
68 study, during expression of an azodyrecin BGC into *S. albidoflavus* J1074<sup>29</sup>, we serendipitously  
69 noticed the production of an unknown alkaloid (**1**). In this study, we link the production of this  
70 novel alkaloid, which we named maramycin (**1**), belonging to the isoquinolinequinone family,  
71 to the heterologous expression of a putative-bifunctional indole prenyltransferase /tryptophan  
72 indole-lyase. Furthermore, we describe isolation, structure elucidation and biological activities  
73 of maramycin (**1**).

74

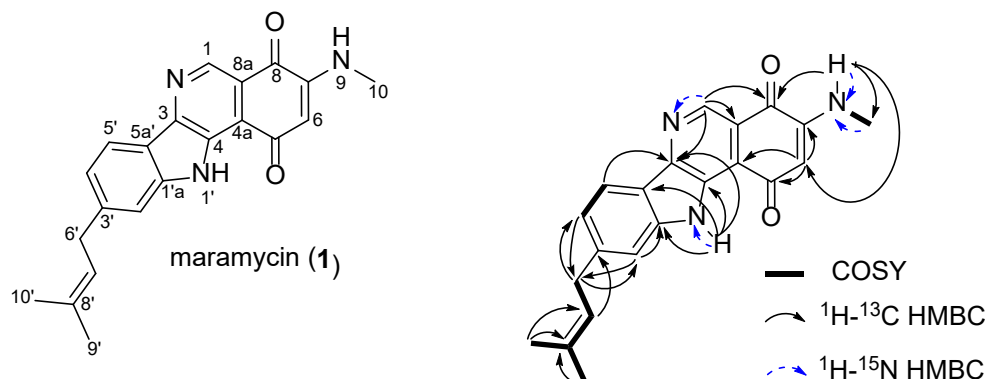
## 75 **Results and Discussion**

### 76 **Production of maramycin, a novel isoquinolinequinone terpenoid through heterologous 77 expression of *mara1***

78 In our recent study on the biosynthesis of azodyrecins<sup>29</sup>, we heterologously expressed a  
79 putative *azd* BGC for cluster validation. Untargeted metabolomic analysis of LC-MS data  
80 revealed the production of a novel metabolite (**1**) that was not detected in the control strain not  
81 carrying the BGC (**Figure S1**). Detailed analysis of HRESIMS data revealed a molecular  
82 formula C<sub>21</sub>H<sub>19</sub>N<sub>3</sub>O<sub>2</sub> for **1**, with a double bond equivalent (DBE) of 14. Analysis of its UV  
83 spectrum and MS/MS fragmentation pattern (**Figure S2**) suggested that **1** was unrelated to the

84 biosynthesis of the azodyrecins (DBE = 3). It was unclear if an induced production of  
85 azodyrecin in the heterologous host has activated cryptic BGC in *S. albidoflavus* J1074<sup>22</sup> or  
86 there was interplay between native and heterologous enzymes resulting in the production of **1**.  
87 To elucidate the structure of the novel alkaloid **1**, *S. albidoflavus* J1074 bearing the *azd* BGC  
88 was cultivated on 5 L of solid agar and extracted using ethyl acetate. Following various  
89 isolation and purification steps, **1** was obtained and characterized by detailed NMR (**Table S1**)  
90 and MS analysis. Compound **1** was isolated as a red amorphous powder. The 1D <sup>13</sup>C (**Figure S3**),  
91 2D <sup>1</sup>H-<sup>13</sup>C edited-HSQC and HMBC (**Figure S4**) spectra identified 21 carbon signals,  
92 including three methyl groups, a methylene, six methine groups, and eleven quartenary carbons.  
93 The <sup>1</sup>H NMR spectrum (**Figure S5**) of **1** showed signals from three methyl groups [ $\delta_{\text{H}}$  1.75  
94 (6H) and 2.84], one methylene appearing as a doublet, six  $\text{sp}^2$  methines, and two exchangeable  
95 protons belonging to NH groups ( $\delta_{\text{H}}$  7.86 and 11.91); the latter two signals were confirmed by  
96 HSQC and <sup>1</sup>H-<sup>15</sup>N HMBC (**Figure S6**) experiments. These data indicated that compound **1**  
97 belonged to the isoquinolinonequinone class of compounds. Furthermore, the methine proton  
98 resonances appearing as singlets at  $\delta_{\text{H}}$  8.97 and 5.69, together with the signals of NH at  $\delta_{\text{H}}$  7.86  
99 and the methyl doublet at  $\delta_{\text{H}}$  2.84 were characteristics of mansouramycins<sup>18</sup>, a group of  
100 isoquinolinonequinones previously isolated from a marine *Streptomyces*<sup>18</sup>. Following literature  
101 reviews and spectroscopic data comparison, the NMR data of **1** were found to be similar to  
102 those of mansouramycin E<sup>18</sup>, except for the presence of an additional prenyl unit in **1**, and that  
103 an aromatic methine in mansouramycin E was present as a quartenary carbon (C-3') in **1**. The  
104 presence and position of an additional prenyl group was established following 2D NMR data  
105 analysis (**Figure 1**); for instance, COSY (**Figure S7**) correlations between CH<sub>2</sub>-6' and CH-7'  
106 together with HMBC correlations from both H-9' and H-10' to C-8' and C-7'. Further HMBC  
107 correlation from H-7' to C-3' positioned the prenyl moiety on C-3'. The remaining structure of

108 **1** was further confirmed by detailed HMBC data (**Figure S8**) analysis. Hence, the structure of  
109 **1** was established as a new isoquinolinequinone terpenoid and named maramycin (**1**).



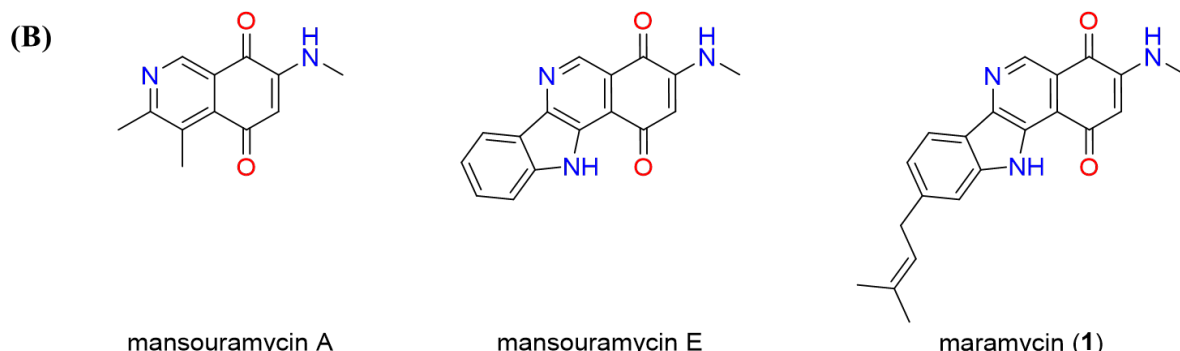
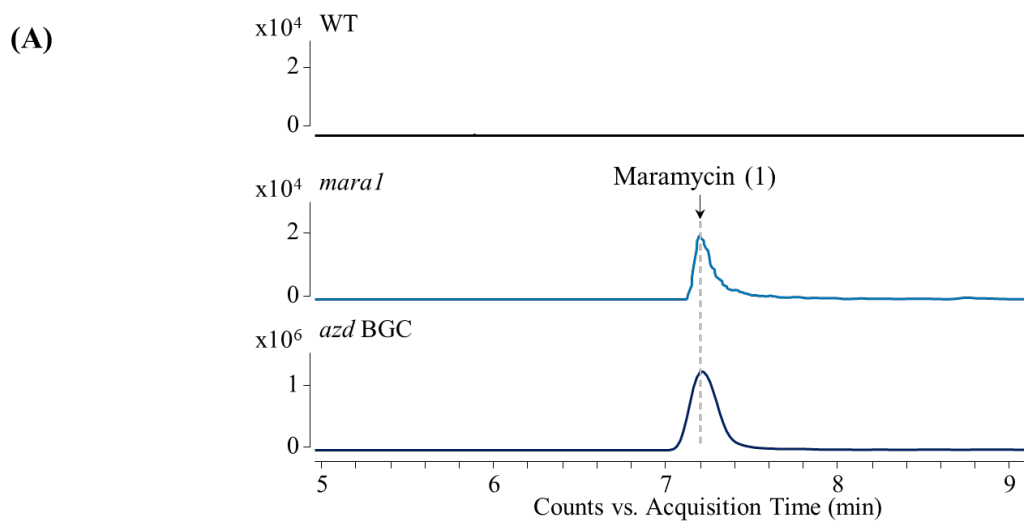
110

111 **Figure 1.** Chemical structure of isoquinolinequinone terpenoid maramycin (**1**) and selected 2D  
112 NMR correlations important for the structure elucidation.

113

#### 114 **Biosynthesis of maramycin**

115 Mansouramycins are encoded by *man* BGC<sup>23</sup> in *S. albidoflavus* J1074, which has been  
116 characterized through gene inactivation and heterologous expression experiments, showing  
117 that *mans3-9* are essential genes for mansouramycin biosynthesis<sup>23</sup>. There have been no  
118 previous reports on natural prenylated mansouramycins and there are no adjacent  
119 prenyltransferase enzymes in *S. albidoflavus* J1074 associated with the *man* BGC. Given the  
120 distinctive prenyl group present in **1**, we reexamined the cloned *azd* BGC region and identified  
121 a candidate gene (*maral*). The putative Maral1 enzyme contained an indole prenyltransferase  
122 domain<sup>30</sup> and a tryptophan indole-lyase domain<sup>31</sup>. To confirm its function, expression of just  
123 *maral* in *S. albidoflavus* J1074 indeed resulted in the production of maramycin (**1**) (**Figure**  
124 **2.A**).



125

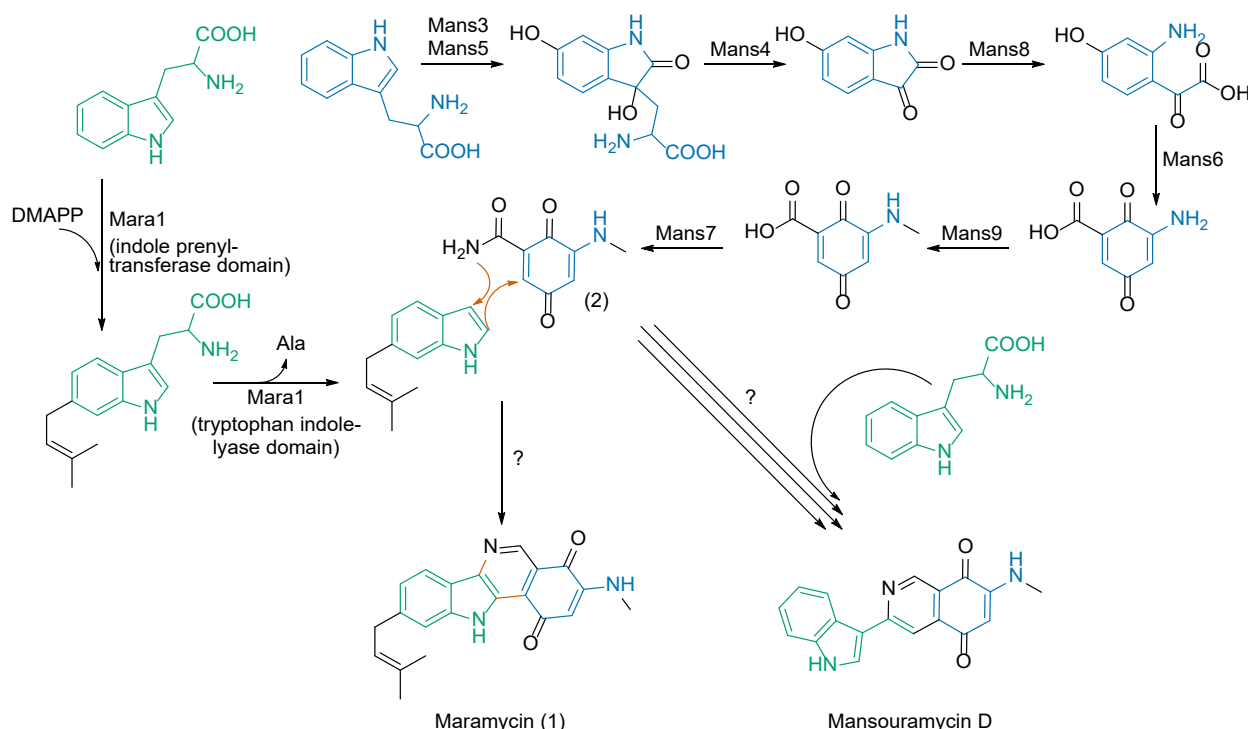
126 **Figure 2.** (A) Extracted ion chromatogram ( $[\text{M}+\text{H}]^+ = 346.1550 \pm 10 \text{ ppm}$ ) of maramycin (1)  
127 from LC-MS samples of *Streptomyces albidoflavus* J1074 (WT) and two mutant strain samples  
128 expressing *maral* and *azd* BGC, respectively. (B) Structures of mansouramycins A<sup>32</sup> and E<sup>22</sup>,  
129 and maramycin (1).

130

131 Due to the high structural similarity to the mansouramycins, we hypothesize that maramycin  
132 was synthesized in combination of the native *man* BGC and the foreign *maral* gene. The *man*  
133 BGC produces 2, an intermediate for mansouramycin which we believe reacts with the  
134 prenylated indole product of Mara1 (**Figure 3**). Mara1 is a bifunctional enzyme which could  
135 catalyze the conversion of tryptophan into a prenylated indole. Firstly, a tryptophan is  
136 prenylated at the C-3' position by the indole prenyltransferase, subsequently the tryptophan  
137 indole-lyase domain facilitates a  $\beta$ -elimination reaction producing the prenylated indole

138 precursor 6-(3-methyl-2-butenyl)-indole. This prenylated indole is then incorporated into the  
139 quinone intermediate to form maramycin (1).

140



141  
142 **Figure 3.** Proposed biosynthesis pathway of maramycin (1), where Mara1 is responsible for  
143 formation of 6-(3-methyl-2-butenyl)-indole which reacts with mansouramycin biosynthesis  
144 intermediate, 5-(methylamino)-3,6-dioxocyclohexa-1,4-diene-1-carboxamide (2), formed by  
145 Mans7 to form maramycin (1).

146

### 147 **Mara1: A rare bifunctional enzyme**

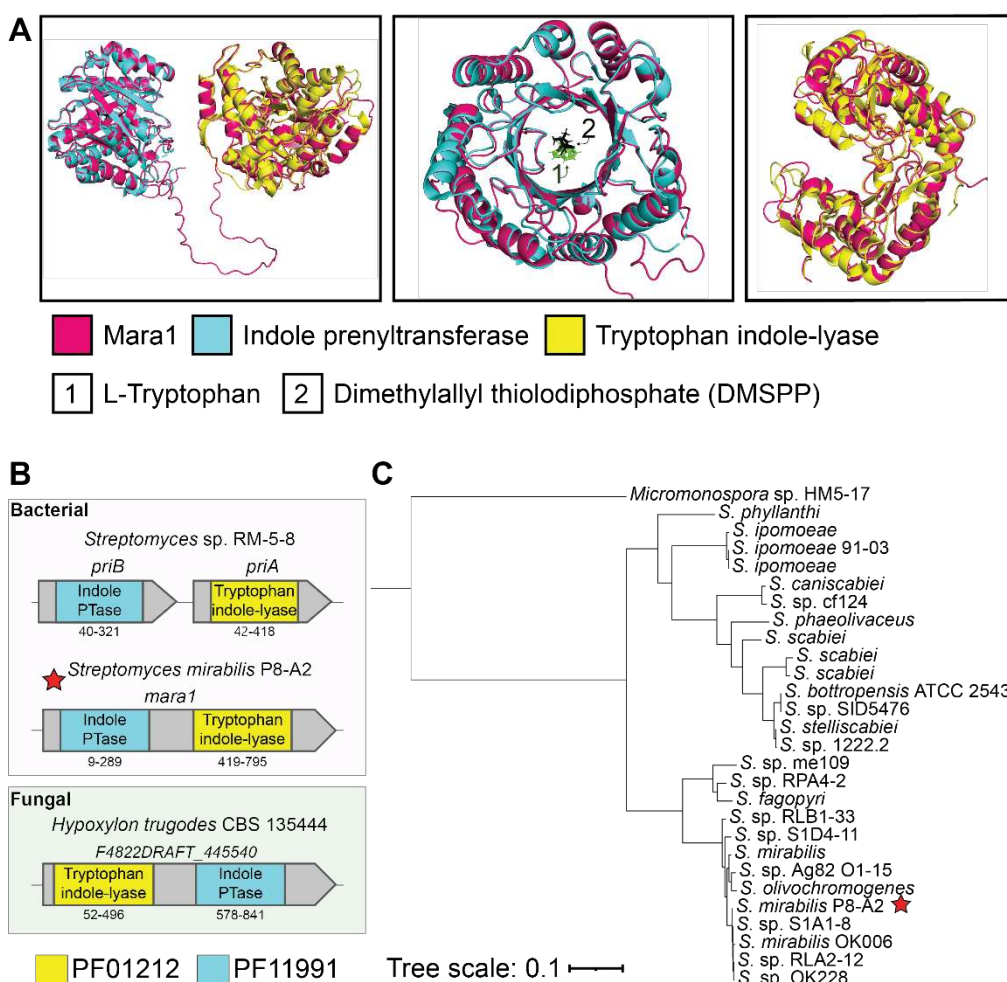
148 The Mara1 enzymatic structure was assessed by comparing an AlphaFold protein model<sup>33,34</sup> to  
149 crystal structures available in the Protein Data Bank (PDB) using FoldSeek<sup>35</sup>. This analysis  
150 confirmed the similarity of the Mara1 N-terminus to the prenyltransferase, PriB, (PDB: 5INJ,  
151 898 MatchAlign score, 0.923 Root Mean Square Deviation “RMSD”)<sup>36</sup> and the C-terminus to  
152 Tryptophan indole-lyase (PDB: 5W1B, 1672 MatchAlign score, 0.745 RMSD)<sup>37</sup>. These

153 alignment scores demonstrate high structural congruence between the two distinct domains and  
154 the fused Mara1 enzyme (**Figure 4.A**).

155

156 To investigate the prevalence of other proteins with similar fused domain architecture we  
157 queried the Interpro database (v 96.0) for proteins containing the Pfam domains 11991 (indole-  
158 prenyltransferase) and Pfam 01212 (tryptophan indole-lyase). Our query produced two distinct  
159 families of proteins: one bacterial (29 hits) and one fungal (30 hits). The bacterial family was  
160 almost exclusively found in *Streptomyces*, apart from a single homologue found in the  
161 taxonomically distinct but related genus *Micromonospora*. These proteins featured a N-  
162 terminal indole prenyltransferase domain followed by C-terminal tryptophan indole-lyase  
163 domain. Interestingly, the fungal enzymes displayed a reversed domain order, with the  
164 tryptophan indole-lyase at the N-terminus (**Figure 4.B**). Analysis using the antiSMASH  
165 database (v4)<sup>38</sup> identified the bacterial bifunctional enzyme in 28 biosynthetic regions  
166 (*Micromonospora* sp. HM5-17 not present antiSMASH database v4). Further 156 regions  
167 contained the two domains as separate, adjacent enzymes, all of which maintained the  
168 sequential domain order seen in the Mara1 bifunctional enzyme. This separate gene  
169 architecture is also observed in the PriB containing BGC responsible for 5-isoprenylindole-3-  
170 carboxylate  $\beta$ -D-glycosyl ester production<sup>39</sup> (MiBIG: BGC0001483) and the isatin-type  
171 antibiotic 7-prenylisatin<sup>40</sup> (MiBIG: BGC0001294) (**Figure 4.B**). In both BGCs these domains  
172 act together to produce a prenylated indole structure from a tryptophan precursor. *Streptomyces*  
173 strains containing this enzyme are closely related, suggesting a potential recent gene fusion  
174 event producing this novel Mara1 enzyme (**Figure 4.C**).

175



186 **Cytotoxicity of maramycin**

187 Isoquinolinequinones have been reported to be potential anticancer drug candidates<sup>41</sup>. The  
188 effects of maramycin (**1**) on cell viability and proliferation were assessed using various prostate  
189 cancer cell lines. Exposure to maramycin (10  $\mu$ M) for 72 h, inhibited cell growth of LNCaP  
190 and C4-2B cells, by 77.9% and 64.1%, respectively (**Figure S9.A and S9.B, respectively**).  
191 This was caused by moderate cytotoxicity elicited by exposure to **1** which showed IC<sub>50</sub> values  
192 of 11.8  $\mu$ M and 18.4  $\mu$ M, against LNCaP and C4-2B cells, respectively (**Figure S9.E**). Drug  
193 resistance remains the main limiting factor for drug efficacy in cancer treatment. Like for  
194 antimicrobial resistance, reduction of the intracellular concentration of a drug by enhancement  
195 of drug efflux from cells, is a key mechanism of resistance. Therefore, we evaluated the effect  
196 of maramycin on the multi-drug resistant sublines LNCaP<sup>R</sup> and C4-2B<sup>R</sup>, which overexpress  
197 the ABCB1/P-glycoprotein (P-gp) efflux pump and found it to exert comparable levels of cell  
198 growth inhibition in these cells (**Figures S8.C and S8.D**), suggesting it can evade Pgp-  
199 mediated multidrug resistance. Maramycin does not appear to have antibacterial properties  
200 against drug resistant Gram-negative pathogens. When *S. albidoflavus* J1074 WT and *S.*  
201 *albidoflavus* J1074 bearing the *azd* BGC were co-cultured against multidrug-resistant strains  
202 of *Actinetobacter baumannii* and *Escherichia coli*, no inhibition zone was observed.

203

204 **Conclusion**

205 In this study we discovered and characterized maramycin, a novel alkaloid with promising  
206 anticancer activity. The production of this compound arose from cross-talk of a rare  
207 bifunctional prenyltransferase/tryptophan indole lyase, capable of generating prenylated  
208 indoles from a tryptophan, and native mansouramycin biosynthesis. We believe this enzyme  
209 has wide applicability to rationally engineer tryptophan derived natural products and to create  
210 promising novel analogues.

211 **Methods**

212 **General Experimental Procedures.** Optical rotations were recorded on an AUTOPOL III -  
213 S2 Dual Wavelength (589/546 nm) Automatic Polarimeter (Rudolph Research Analytical). IR  
214 data were acquired on Bruker Alpha FTIR spectrometer using OPUS version 7.2. The NMR  
215 spectra were recorded on a Bruker AVANCE III 800 MHz spectrometer equipped with a 5 mm  
216 TCI CryoProbe using standard pulse sequences. The  $^1\text{H}$  and  $^{13}\text{C}$  NMR chemical shifts were  
217 referenced to the residual solvent signals at  $\delta_{\text{H}}$  2.50,  $\delta_{\text{C}}$  39.52 ppm for for DMSO-*d*6. UHPLC-  
218 HRMS was performed on an Agilent Infinity 1290 UHPLC system equipped with a diode array  
219 detector. UV-vis spectra were recorded from 190 to 640 nm. All solvents and chemicals used  
220 for HRMS, and chromatography were LC-MS grade, while the solvents for metabolite  
221 extraction were of HPLC grade. Water was purified using a Milli-Q system.

222

223 **LC-ESI-HRMS/MS Analysis.** Ultra-high-performance liquid chromatography-diode array  
224 detection-quadrupole time-of-flight mass spectrometry (UHPLC-DAD-QTOFMS) was  
225 performed on an Agilent Infinity 1290 UHPLC system (Agilent Technologies, Santa Clara, CA,  
226 USA) equipped with a diode array detector. Separation was achieved on a  $150 \times 2.1$  mm i.d.,  
227 1.9  $\mu\text{m}$ , Poroshell 120 Phenyl Hexyl column (Agilent Technologies, Santa Clara, CA) held at  
228 40°C. The sample (1  $\mu\text{L}$ ) was eluted at a flow rate of  $0.35 \text{ mL min}^{-1}$  using a linear gradient  
229 from 10% acetonitrile (LC-MS grade) in Milli-Q water buffered with 20 mM formic acid  
230 increasing to 100% in 10 min, staying there for 2 min before returning to 10% in 0.1 min.  
231 Starting conditions were held for 3 min before the following run.

232 Mass spectrometry (MS) detection was performed on an Agilent 6545 QTOF MS equipped  
233 with Agilent Dual Jet Stream electrospray ion source (ESI) with a drying gas temperature of  
234 250°C, a gas flow of  $8 \text{ L min}^{-1}$ , sheath gas temperature of 300°C and flow of  $12 \text{ L min}^{-1}$

235 Capillary voltage was set to 4000 V and nozzle voltage to 500 V in positive mode. Mass spectra  
236 were recorded as centroid data, at an  $m/z$  of 100–1700, and auto MS/HRMS fragmentation was  
237 performed at three collision energies (10, 20, and 40 eV), on the three most intense precursor  
238 peaks per cycle. The acquisition rate was 10 spectra  $s^{-1}$ . Data were handled using Agilent  
239 MassHunter Qualitative Analysis software (Agilent Technologies, Santa Clara, CA). Lock  
240 mass solution in 70 % MeOH in water was infused in the second sprayer using an extra LC  
241 pump at a flow of 15  $\mu L\ min^{-1}$  using a 1:100 splitter. The solution contained 1  $\mu M$  tributylamine  
242 (Sigma-Aldrich) and 10  $\mu M$  Hexakis (2, 2, 3, 3-tetrafluoropropoxy) phosphazene (Apollo  
243 Scientific Ltd., Cheshire, UK) as lock masses. The  $[M + H]^+$  ions ( $m/z$  186.2216 and 922.0098,  
244 respectively) of both compounds were used.

245

246 **Microbial strains and culture conditions.** *Escherichia coli* ET12567/pUZ8002<sup>42,43</sup>,  
247 *Escherichia coli* Mach1 (Thermo Fisher Scientific), *Streptomyces albidoflavus* J1074<sup>25</sup> and  
248 *Streptomyces albidoflavus* J1074  $\Phi$ C31::pAzd<sup>29</sup>. All *Escherichia coli* strains were grown in  
249 liquid/solid LB medium (5.0 g/L yeast extract, 10.0 g/L peptone, 10.0 g/L NaCl) at 37 °C.  
250 *Streptomyces albidoflavus* was grown on SFM (20.0 g/L fat reduced soy flour (fettreduziert  
251 Bio Sojamehl; Hensel, Germany)), 20.0 g/L D-mannitol (Sigma-Aldrich), and 1.0 L tap water  
252 (Kgs. Lyngby, Denmark)) or ISP2 (yeast extract 4g/L (Thermo Fisher Scientific), malt extract  
253 10g/L (Sigma-Aldrich), glucose 4g/L (Sigma-Aldrich), 1.0 L deionized water) at 30 °C. For  
254 conjugations, SFM media was supplemented to contain final concentration of 10 mM MgCl<sub>2</sub>.  
255 Appropriate antibiotics were supplemented with the following working concentrations: 100  
256  $\mu$ g/mL apramycin sulfate (Sigma-Aldrich), 25  $\mu$ g/mL chloramphenicol (Sigma-Aldrich), 50  
257  $\mu$ g/mL kanamycin sulphate (Sigma-Aldrich) and 25  $\mu$ g/mL nalidixic acid (Sigma-Aldrich).

258

259 **Heterologous expression of *mara1* in *S. albidoflavus* J1074.** All polymerase chain reactions  
260 were performed using Q5 High-Fidelity 2X Master Mix (New England Biolabs) and all primers  
261 were synthesized by IDT (Integrated DNA Technologies). PCR amplification of pRM4e<sup>44</sup> was  
262 performed using matmal0292: “GCGAGTGTCCGTTGAG” and matmal0293:  
263 “ATGGACGTCCCCTTCCT”, while *mara1* was amplified by primer extension PCR using  
264 matmal0294: “actcgaacggacactcgccTAGACGGTCACCGGCTG” and matmal0296:  
265 “caggaagggacgtccatATGATCACCTCCGTCCAGG”. The PCR products of expected 5.4  
266 kbp and 2.6 kbp size, respectively, were gel purified using NucleoSpin Gel and PCR Clean-up  
267 (Macherey-Nagel) kit according to suppliers' instructions. The *mara1* fragment was cloned into  
268 pRM4e vector using NEBuilder HiFi DNA Assembly (New England Biolabs) master mix and  
269 introduced into *E. coli* Mach1 by heat shock method<sup>45,46</sup>. The obtained plasmid, pRM4e-*mara1*  
270 (**Figure S10**), was verified via colony PCR, expected fragment size 3.1 kbp, and subsequent  
271 Sanger sequencing (Eurofins Genomics) using matmal0208:  
272 “GTCTGTCGAGAAGTTCTGATC” and matmal0209:  
273 “ACATGTTCTTCCTGCCTTATC”. The acquired plasmid was purified using NucleoSpin  
274 Plasmid EasyPure (Macherey-Nagel) kit according to suppliers instructions, cloned into *E. coli*  
275 ET12567/pUZ8002 and introduced into *S. albidoflavus* J1074 via conjugation. The resulting  
276 apramycin resistant clones were selected for LC-MS analysis.

277  
278 **Bacterial cultivation** A seed culture was prepared by inoculating spores of strain *S.*  
279 *albidoflavus* J1074  $\Phi$ C31::pAzd into a baffled conical flask containing 50 mL of liquid ISP2  
280 medium and incubated at 30 °C overnight with constant shaking at 180 rpm. The seed culture  
281 was inoculated on ISP2 agar plates and incubated at 30 °C for 7 days in the dark. A total of 5  
282 L (200 plates) of ISP2 agar were prepared for extraction and isolation of maramycin.

283

284 **Extraction and isolation of maramycin.** The agar cultures were sliced into small pieces and  
285 extracted under sonication for 30 min with EtOAc (2 x 5 L). The EtOAc was filtered and  
286 removed under reduced pressure using rotary evaporator to yield 599 mg of crude extract. The  
287 extract was subjected to flash chromatography using a C<sub>18</sub>-bonded Si-gel cartridge (Biotage  
288 SNAP 50 g) on Biotage Isolera Flash Chromatography system, eluted with step-gradient  
289 solvent systems (10% MeOH/H<sub>2</sub>O to 100% MeOH; 10% increment; 132 mL each) at a flow  
290 rate of 30 mL/min to give 20 fractions (66 mL each). Fractions 14–20 were combined following  
291 HRMS analysis that suggested the presence of the isoquinolinquinone terpenoid. The combined  
292 fraction was further purified using RP-HPLC column (Luna 5  $\mu$ m C<sub>18</sub>-Phenomenex, 100  $\text{\AA}$ ,  
293 250 x 10 mm) with a linear gradient of 45%–85% ACN/H<sub>2</sub>O in 20 min to afford maramycin  
294 (**1**, 1.1 mg).

295

## 296 **Bioinformatic analysis of bifunctional enzyme**

297 The *mara1* sequence is identical to already existing model AF-A0A856NK67-F1-model\_v4 in  
298 the AlphaFold database<sup>33,34</sup>. Structurally similar models were identified in the PDB using  
299 FoldSeek<sup>35</sup>. The similarity of identified matches to Mara1 were assessed by performing  
300 PyMOL “super” structure alignment. The BGC annotation tool antiSMASH 7.0.0<sup>47</sup> was used  
301 to annotate the *mara1* gene and identify relevant Pfam domains. To identify further proteins  
302 containing both Pfam 01212 ( $\beta$ -eliminating lyase) and Pfam 11991 (tryptophan  
303 dimethylallyltransferase) domains, the InterPro database (v 96.0) was queried via the domain  
304 search. The 29 amino sequences of identified bacterial proteins were downloaded and aligned  
305 with MAFFT (v 7.490) using the --auto flag and model L-INS-I<sup>48</sup>. Phylogenetic trees were then  
306 constructed using FastTree2 (v 2.1.11)<sup>49</sup> and visualized and annotated in iTol (v 6)<sup>50</sup>. To  
307 identify enzymes in other biosynthetic gene clusters the amino acid sequence was queried  
308 against the antiSMASHdb (v4)<sup>51</sup>.

309

310 **Cell growth and cytotoxicity assay**

311 Two prostate cancer cell lines, LNCaP and C4-2B, as well as the drug-resistant derivative  
312 sublines, LNCaP<sup>R</sup> and C4-2B<sup>R</sup>, respectively<sup>52</sup>, were used to evaluate the effect of maramycin  
313 on cell viability and proliferation. All cell lines were cultured and maintained in RPMI-1640  
314 medium + glutaMAX™-I (Gibco, Invitrogen, Carlsbad, CA, United States) supplemented with  
315 10% fetal bovine serum (FBS). One day prior to drug exposure measurements, cells were  
316 seeded into 6-well plates at a density of  $0.3 \times 10^6$  cells/well. On the next day, the medium in  
317 each well was replaced with 2mL of fresh warm medium containing either 10  $\mu$ M of  
318 maramycin or vehicle. Cell proliferation dynamics were monitored in real-time using a lens-  
319 free Cellwatcher microscopy device (PHIO, Germany). The cell growth curves were generated  
320 with the analysis module available from PHIO to determine the total area covered by cells.  
321 Cytotoxicity was evaluated using the CellTox Green Cytotoxicity Assay kit (Promega,  
322 Madison, WI, USA) after 48h of exposure to various concentrations of maramycin ( $10^{-7}$  M to  
323  $2 \times 10^{-5}$  M), according to manufacturer's instructions. Briefly, CellTox green cytotoxicity  
324 reagent was added to the media at a final concentration of 1X, and the relative cytotoxicity was  
325 calculated relative to the control well treated with vehicle. The drug concentrations that caused  
326 inhibition of 50% cell viability (IC<sub>50</sub>) were determined from the dose-response curves. Curve  
327 fitting and analyses using non-linear regression models were performed using GraphPad Prism  
328 version 10.0.0 for Windows (GraphPad Software, Boston, MA, USA).

329

330 ***Maramycin (1)***

331 Red amorphous powder; UV (CH<sub>3</sub>CN/H<sub>2</sub>O)  $\lambda_{\text{max}}$  236 (100%), 270 (50%), 390 (25%) nm; IR  
332 (ATR)  $\nu_{\text{max}}$  3306, 2943, 2801, 2023, 1449, 1409, 1120, 1020, 623 cm<sup>-1</sup>; <sup>1</sup>H and <sup>13</sup>C NMR see

333 Supporting Information (Table S1); (+)-HRESIMS  $m/z$  346.1564 [M+H]<sup>+</sup> (calcd for  
334 C<sub>21</sub>H<sub>20</sub>N<sub>3</sub>O<sub>2</sub>, 346.1550).

335

336 **Data availability**

337 MassIVE MSV000093927, Genome sequence data for *Streptomyces mirabilis* P8-A2 is  
338 available under the NCBI RefSeq accession NZ\_JARAKF000000000.1.

339

340 **Supporting Information**

341 Additional details on the HPLC traces of heterologous expression strain, NMR data of  
342 maramycin, bioactivity data and plasmid map for heterologous expression of Mara1.

343

344 **Acknowledgements**

345 This study was supported by the Danish National Research Foundation (DNRF137) as part of  
346 the Center for Microbial Secondary Metabolites (CeMiSt). S.E.W. would furthermore  
347 acknowledge funding by the Novo Nordisk Foundation Postdoctoral Fellowship  
348 (NNF22OC0079021). T.W. would furthermore acknowledge funding by the Novo Nordisk  
349 Foundation (NNF20CC0035580, NNF16OC0021746). The NMR Center DTU and the Villum  
350 Foundation are acknowledged for access to the 800 MHz spectrometer.

351

352 The metabolomic data was generated at DTU Metabolomics Core facilities with help of A.  
353 Andersen.

354

355 **Author contributions**

356 M.M., M.W., S.E.W set out the methodology of the study, performed data collection,  
357 conducted bioinformatic data curation, conducted data analysis and produced visualizations for

358 the manuscript. M.M, M.W., S.E.W. wrote the original draft of the manuscript with help from  
359 C.H.G., R.S., L.D.O.S., M.S.C., P.C., J.M.A.M., T.W., L.D. All authors reviewed and edited  
360 the manuscript. T.W. and L.D. conceived the project, provided supervision and acquired  
361 funding. All authors have read and agreed to the published version of the manuscript.

362

### 363 **Reference**

364 (1) WHO. *Model List of Essential Medicines – 23rd List, 2023. In: The Selection and Use of*  
365 *Essential Medicines 2023: Executive Summary of the Report of the 24th WHO Expert*  
366 *Committee on the Selection and Use of Essential Medicines, 24 – 28 April 2023. Geneva:*  
367 *World Health Organization; 2023 (WHO/MHP/HPS/EML/2023.02). Licence: CC BYNC-SA 3.0*  
368 *IGO.; 2023.*

369 (2) Van Keulen, G.; Dyson, P. J. Production of Specialized Metabolites by Streptomyces Coelicolor  
370 A3(2). *Adv Appl Microbiol* **2014**, *89*, 217–266. <https://doi.org/10.1016/B978-0-12-800259-9.00006-8>.

372 (3) Ohnishi, Y.; Ishikawa, J.; Hara, H.; Suzuki, H.; Ikenoya, M.; Ikeda, H.; Yamashita, A.; Hattori,  
373 M.; Horinouchi, S. Genome Sequence of the Streptomycin-Producing Microorganism  
374 *Streptomyces Griseus IFO 13350. J Bacteriol* **2008**, *190* (11), 4050–4060.  
375 [https://doi.org/10.1128/JB.00204-08/SUPPL\\_FILE/JB204-08SUPPLEMENT.PDF](https://doi.org/10.1128/JB.00204-08/SUPPL_FILE/JB204-08SUPPLEMENT.PDF).

376 (4) Ikeda, H.; Ishikawa, J.; Hanamoto, A.; Shinose, M.; Kikuchi, H.; Shiba, T.; Sakaki, Y.; Hattori,  
377 M.; Omura, S. Complete Genome Sequence and Comparative Analysis of the Industrial  
378 Microorganism *Streptomyces avermitilis*. *Nature Biotechnology* **2003** *21*:5 **2003**, *21* (5), 526–  
379 531. <https://doi.org/10.1038/nbt820>.

380 (5) Bentley, S. D.; Chater, K. F.; Cerdeño-Tárraga, A. M.; Challis, G. L.; Thomson, N. R.; James, K.  
381 D.; Harris, D. E.; Quail, M. A.; Kieser, H.; Harper, D.; Bateman, A.; Brown, S.; Chandra, G.;  
382 Chen, C. W.; Collins, M.; Cronin, A.; Fraser, A.; Goble, A.; Hidalgo, J.; Hornsby, T.; Howarth, S.;  
383 Huang, C. H.; Kieser, T.; Larke, L.; Murphy, L.; Oliver, K.; O’Neil, S.; Rabbinowitsch, E.;  
384 Rajandream, M. A.; Rutherford, K.; Rutter, S.; Seeger, K.; Saunders, D.; Sharp, S.; Squares, R.;  
385 Squares, S.; Taylor, K.; Warren, T.; Wietzorrekk, A.; Woodward, J.; Barrell, B. G.; Parkhill, J.;  
386 Hopwood, D. A. Complete Genome Sequence of the Model Actinomycete *Streptomyces*  
387 *Coelicolor A3(2)*. *Nature* **2002** *417*:6885 **2002**, *417* (6885), 141–147.  
388 <https://doi.org/10.1038/417141a>.

389 (6) Lee, N.; Hwang, S.; Lee, Y.; Cho, S.; Palsson, B.; Cho, B. K. Synthetic Biology Tools for Novel  
390 Secondary Metabolite Discovery in *Streptomyces*. *J. Microbiol. Biotechnol.* **2019**, *29* (5), 667–  
391 686. <https://doi.org/10.4014/JMB.1904.04015>.

392 (7) Baral, B.; Akhgari, A.; Metsä-Ketelä, M. Activation of Microbial Secondary Metabolic  
393 Pathways: Avenues and Challenges. *Synth Syst Biotechnol* **2018**, *3* (3), 163–178.  
394 <https://doi.org/10.1016/J.SYNBIO.2018.09.001>.

395 (8) Luo, Y.; Huang, H.; Liang, J.; Wang, M.; Lu, L.; Shao, Z.; Cobb, R. E.; Zhao, H. Activation and  
396 Characterization of a Cryptic Polycyclic Tetramate Macrolactam Biosynthetic Gene Cluster.  
397 *Nature Communications* 2013 4:1 **2013**, 4 (1), 1–8. <https://doi.org/10.1038/ncomms3894>.

398 (9) Young, T. S.; Walsh, C. T. Identification of the Thiazolyl Peptide GE37468 Gene Cluster from  
399 Streptomyces ATCC 55365 and Heterologous Expression in Streptomyces Lividans. *Proc Natl  
400 Acad Sci U S A* **2011**, 108 (32), 13053–13058.  
401 [https://doi.org/10.1073/PNAS.1110435108/SUPPL\\_FILE/APPENDIX.PDF](https://doi.org/10.1073/PNAS.1110435108/SUPPL_FILE/APPENDIX.PDF).

402 (10) Covington, B. C.; Seyedsayamdost, M. R. MetEx, a Metabolomics Explorer Application for  
403 Natural Product Discovery. *ACS Chem Biol* **2021**, 16 (12), 2825–2833.  
404 [https://doi.org/10.1021/ACSCHEMbio.1C00737/SUPPL\\_FILE/CB1C00737\\_SI\\_001.PDF](https://doi.org/10.1021/ACSCHEMbio.1C00737/SUPPL_FILE/CB1C00737_SI_001.PDF).

405 (11) Wakefield, J.; Hassan, H. M.; Jaspars, M.; Ebel, R.; Rateb, M. E. Dual Induction of New  
406 Microbial Secondary Metabolites by Fungal Bacterial Co-Cultivation. *Front Microbiol* **2017**, 8  
407 (JUL). <https://doi.org/10.3389/FMICB.2017.01284>.

408 (12) Milanowski, D. J.; Gustafson, K. R.; Kelley, J. A.; McMahon, J. B. Caulibugulones A-F, Novel  
409 Cytotoxic Isoquinoline Quinones and Iminoquinones from the Marine Bryozoan Caulibugula  
410 Intermis. *J Nat Prod* **2004**, 67 (1), 70–73.  
411 <https://doi.org/10.1021/NP030378L/ASSET/IMAGES/LARGE/NP030378LF1.jpeg>.

412 (13) Choi, Y. H.; Park, A.; Schmitz, F. J.; van Altena, I. Perfragilins A and B, Cytotoxic  
413 Isoquinolinequinones from the Bryozoan Membranipora Perfragilis. *J Nat Prod* **1993**, 56 (8),  
414 1431–1433. <https://doi.org/10.1021/NP50098A032>.

415 (14) Pettit, G. R.; Knight, J. C.; Collins, J. C.; Herald, D. L.; Pettit, R. K.; Boyd, M. R.; Young, V. G.  
416 Antineoplastic Agents 430. Isolation and Structure of Cribrostatins 3, 4, and 5 from the  
417 Republic of Maldives Cribrochalina Species. *J Nat Prod* **2000**, 63 (6), 793–798.  
418 [https://doi.org/10.1021/NP990618Q/SUPPL\\_FILE/NP990618Q\\_S.PDF](https://doi.org/10.1021/NP990618Q/SUPPL_FILE/NP990618Q_S.PDF).

419 (15) Frincke, J. M.; Faulkner, D. J. Antimicrobial Metabolites of the Sponge Reniera Sp. *J Am Chem  
420 Soc* **1982**, 104 (1), 265–269.  
421 [https://doi.org/10.1021/JA00365A048/ASSET/JA00365A048.FP.PNG\\_V03](https://doi.org/10.1021/JA00365A048/ASSET/JA00365A048.FP.PNG_V03).

422 (16) Kim, Y. N.; Ji, Y. K.; Kim, N. H.; Tu, N. Van; Rho, J. R.; Jeong, E. J. Isoquinolinequinone  
423 Derivatives from a Marine Sponge (Haliclona Sp.) Regulate Inflammation in In Vitro System of  
424 Intestine. *Mar Drugs* **2021**, 19 (2). <https://doi.org/10.3390/MD19020090>.

425 (17) Hawas, U. W.; Shaaban, M.; Shaaban, K. A.; Speitling, M.; Maier, A.; Kelter, G.; Fiebig, H. H.;  
426 Meiners, M.; Helmke, E.; Laatsch, H. Mansouramycins A-D, Cytotoxic Isoquinolinequinones  
427 from a Marine Streptomycete. *J Nat Prod* **2009**, 72 (12), 2120–2124.  
428 [https://doi.org/10.1021/NP900160G/SUPPL\\_FILE/NP900160G\\_SI\\_001.PDF](https://doi.org/10.1021/NP900160G/SUPPL_FILE/NP900160G_SI_001.PDF).

429 (18) Shaaban, M.; Shaaban, K. A.; Kelter, G.; Fiebig, H. H.; Laatsch, H. Mansouramycins E-G,  
430 Cytotoxic Isoquinolinequinones from Marine Streptomycetes. *Mar Drugs* **2021**, 19 (12).  
431 <https://doi.org/10.3390/MD19120715>.

432 (19) Chai, S.; Cao, M.; Feng, Z. Identification and Heterologous Expression of an  
433 Isoquinolinequinone Biosynthetic Gene Cluster from Streptomyces Albus J1074. *Biochem  
434 Biophys Res Commun* **2021**, 540, 51–55. <https://doi.org/10.1016/J.BBRC.2020.12.093>.

435 (20) Xu, F.; Nazari, B.; Moon, K.; Bushin, L. B.; Seyedsayamdst, M. R. Discovery of a Cryptic  
436 Antifungal Compound from *Streptomyces Albus* J1074 Using High-Throughput Elicitor  
437 Screens. *J Am Chem Soc* **2017**, 139 (27), 9203–9212.  
438 [https://doi.org/10.1021/JACS.7B02716/ASSET/IMAGES/LARGE/JA-2017-027165\\_0007.jpeg](https://doi.org/10.1021/JACS.7B02716/ASSET/IMAGES/LARGE/JA-2017-027165_0007.jpeg).

439 (21) Huang, C.; Yang, C.; Zhang, W.; Zhu, Y.; Ma, L.; Fang, Z.; Zhang, C. Albumycin, a New  
440 Isoindolequinone from *Streptomyces Albus* J1074 Harboring the Fluostatin Biosynthetic Gene  
441 Cluster. *The Journal of Antibiotics* 2019 72:5 **2019**, 72 (5), 311–315.  
442 <https://doi.org/10.1038/s41429-019-0161-4>.

443 (22) Chai, S.; Cao, M.; Feng, Z. Identification and Heterologous Expression of an  
444 Isoquinolinequinone Biosynthetic Gene Cluster from *Streptomyces Albus* J1074. *Biochem*  
445 *Biophys Res Commun* **2021**, 540, 51–55. <https://doi.org/10.1016/J.BBRC.2020.12.093>.

446 (23) Shuai, H.; Myronovskyi, M.; Rosenkränzer, B.; Paulus, C.; Nadmid, S.; Stierhof, M.; Kolling, D.;  
447 Luzhetsky, A. Novel Biosynthetic Route to the Isoquinoline Scaffold. *ACS Chem Biol* **2022**, 17  
448 (3), 598–608.  
449 [https://doi.org/10.1021/ACSCHEMBIO.1C00869/ASSET/IMAGES/LARGE/CB1C00869\\_0011.JPEG](https://doi.org/10.1021/ACSCHEMBIO.1C00869/ASSET/IMAGES/LARGE/CB1C00869_0011.JPEG).

450 (24) Myronovskyi, M.; Rosenkränzer, B.; Nadmid, S.; Pujic, P.; Normand, P.; Luzhetsky, A.  
451 Generation of a Cluster-Free *Streptomyces Albus* Chassis Strains for Improved Heterologous  
452 Expression of Secondary Metabolite Clusters. *Metab Eng* **2018**, 49, 316–324.  
453 <https://doi.org/10.1016/J.YMBEN.2018.09.004>.

455 (25) Chater, K. F.; Wilde, L. C. Restriction of a Bacteriophage of *Streptomyces Albus* G Involving  
456 Endonuclease Sall. *J Bacteriol* **1976**, 128 (2), 644–650. <https://doi.org/10.1128/JB.128.2.644-650.1976>.

458 (26) Beck, C.; Gren, T.; Ortiz-López, F. J.; Jørgensen, T. S.; Carretero-Molina, D.; Serrano, J. M.;  
459 Tormo, J. R.; Oves-Costales, D.; Kontou, E. E.; Mohite, O. S.; Mingyar, E.; Stegmann, E.;  
460 Genilloud, O.; Weber, T. Activation and Identification of a Griseusin Cluster in *Streptomyces*  
461 Sp. CA-256286 by Employing Transcriptional Regulators and Multi-Omics Methods. *Molecules*  
462 **2021**, Vol. 26, Page 6580 **2021**, 26 (21), 6580. <https://doi.org/10.3390/MOLECULES26216580>.

463 (27) Kontou, E. E.; Gren, T.; Ortiz-López, F. J.; Thomsen, E.; Oves-Costales, D.; Díaz, C.; De La Cruz,  
464 M.; Jiang, X.; Jørgensen, T. S.; Blin, K.; Charusanti, P.; Reyes, F.; Genilloud, O.; Weber, T.  
465 Discovery and Characterization of Epemicins A and B, New 30-Membered Macrolides from  
466 *Kutzneria* Sp. CA-103260. *ACS Chem Biol* **2021**, 16 (8), 1456–1468.  
467 [https://doi.org/10.1021/ACSCHEMBIO.1C00318/ASSET/IMAGES/LARGE/CB1C00318\\_0004.JPEG](https://doi.org/10.1021/ACSCHEMBIO.1C00318/ASSET/IMAGES/LARGE/CB1C00318_0004.JPEG).

469 (28) Oves-Costales, D.; Gren, T.; Sterndorff, E. B.; Martín, J.; Ortiz-López, F. J.; Jørgensen, T. S.;  
470 Jiang, X.; Román-Hurtado, F.; Reyes, F.; Genilloud, O.; Weber, T. Identification and  
471 Heterologous Expression of the Globomycin Biosynthetic Gene Cluster. *Synth Syst Biotechnol*  
472 **2023**, 8 (2), 206–212. <https://doi.org/10.1016/J.SYNBIO.2023.02.001>.

473 (29) Maleckis, M.; Wibowo, M.; Gren, T.; Jarmusch, S. A.; Sterndorff, E. B.; Booth, T.; Henriksen, N.  
474 N. S. E.; Whitford, C. M.; Jiang, X.; Jørgensen, T. S.; Ding, L.; Weber, T. Biosynthesis of the  
475 Azoxy Compound Azodyrecin from *Streptomyces Mirabilis* P8-A2. *ACS Chem Biol* **2024**.  
476 <https://doi.org/10.1021/ACSCHEMBIO.3C00632>.

477 (30) Elshahawi, S. I.; Cao, H.; Shaaban, K. A.; Ponomareva, L. V; Subramanian, T.; Farman, M. L.;  
478 Spielmann, H. P.; Phillips, G. N.; Thorson, J. S.; Singh, S. Structure and Specificity of a  
479 Permissive Bacterial C-Prenyltransferase. *Nat Chem Biol* **2017**, *13* (4), 366–368.  
480 <https://doi.org/10.1038/nchembio.2285>.

481 (31) Mindt, M.; Ferrer, L.; Bosch, D.; Cankar, K.; Wendisch, V. F. De Novo Tryptophanase-Based  
482 Indole Production by Metabolically Engineered *Corynebacterium Glutamicum*. *Appl Microbiol*  
483 *Biotechnol* **2023**, *107* (5), 1621–1634. <https://doi.org/10.1007/s00253-023-12397-4>.

484 (32) Hawas, U. W.; Shaaban, M.; Shaaban, K. A.; Speitling, M.; Maier, A.; Kelter, G.; Fiebig, H. H.;  
485 Meiners, M.; Helmke, E.; Laatsch, H. Mansouramycins A-D, Cytotoxic Isoquinolinequinones  
486 from a Marine Streptomycete. *J Nat Prod* **2009**, *72* (12), 2120–2124.  
487 [https://doi.org/10.1021/NP900160G/SUPPL\\_FILE/NP900160G\\_SI\\_001.PDF](https://doi.org/10.1021/NP900160G/SUPPL_FILE/NP900160G_SI_001.PDF).

488 (33) Jumper, J.; Evans, R.; Pritzel, A.; Green, T.; Figurnov, M.; Ronneberger, O.; Tunyasuvunakool,  
489 K.; Bates, R.; Žídek, A.; Potapenko, A.; Bridgland, A.; Meyer, C.; Kohl, S. A. A.; Ballard, A. J.;  
490 Cowie, A.; Romera-Paredes, B.; Nikolov, S.; Jain, R.; Adler, J.; Back, T.; Petersen, S.; Reiman,  
491 D.; Clancy, E.; Zielinski, M.; Steinegger, M.; Pacholska, M.; Berghammer, T.; Bodenstein, S.;  
492 Silver, D.; Vinyals, O.; Senior, A. W.; Kavukcuoglu, K.; Kohli, P.; Hassabis, D. Highly Accurate  
493 Protein Structure Prediction with AlphaFold. *Nature* **2021** *596*:7873 **2021**, *596* (7873), 583–  
494 589. <https://doi.org/10.1038/s41586-021-03819-2>.

495 (34) Varadi, M.; Anyango, S.; Deshpande, M.; Nair, S.; Natassia, C.; Yordanova, G.; Yuan, D.; Stroe,  
496 O.; Wood, G.; Laydon, A.; Žídek, A.; Green, T.; Tunyasuvunakool, K.; Petersen, S.; Jumper, J.;  
497 Clancy, E.; Green, R.; Vora, A.; Lutfi, M.; Figurnov, M.; Cowie, A.; Hobbs, N.; Kohli, P.;  
498 Kleywegt, G.; Birney, E.; Hassabis, D.; Velankar, S. AlphaFold Protein Structure Database:  
499 Massively Expanding the Structural Coverage of Protein-Sequence Space with High-Accuracy  
500 Models. *Nucleic Acids Res* **2022**, *50* (D1), D439–D444.  
501 <https://doi.org/10.1093/NAR/GKAB1061>.

502 (35) van Kempen, M.; Kim, S. S.; Tumescheit, C.; Mirdita, M.; Lee, J.; Gilchrist, C. L. M.; Söding, J.;  
503 Steinegger, M. Fast and Accurate Protein Structure Search with Foldseek. *Nature*  
504 *Biotechnology* **2023** **2023**, 1–4. <https://doi.org/10.1038/s41587-023-01773-0>.

505 (36) Elshahawi, S. I.; Cao, H.; Shaaban, K. A.; Ponomareva, L. V.; Subramanian, T.; Farman, M. L.;  
506 Spielmann, H. P.; Phillips, G. N.; Thorson, J. S.; Singh, S. Structure and Specificity of a  
507 Permissive Bacterial C-Prenyltransferase. *Nature Chemical Biology* **2017** *13*:4 **2017**, *13* (4),  
508 366–368. <https://doi.org/10.1038/nchembio.2285>.

509 (37) Phillips, R. S.; Buisman, A. A.; Choi, S.; Hussaini, A.; Wood, Z. A. The Crystal Structure of  
510 *Proteus Vulgaris* Tryptophan Indole-Lyase Complexed with Oxindolyl-L-Alanine: Implications  
511 for the Reaction Mechanism. *Acta Crystallogr D Struct Biol* **2018**, *74* (8), 748–759.  
512 <https://doi.org/10.1107/S2059798318003352/LP5034SUP1.PDF>.

513 (38) Blin, K.; Shaw, S.; Medema, M. H.; Weber, T. The AntiSMASH Database Version 4: Additional  
514 Genomes and BGCs, New Sequence-Based Searches and More. *Nucleic Acids Res* **2013**, *1*  
515 (1256879), 13–14. <https://doi.org/10.1093/NAR/GKAD984>.

516 (39) Wang, X.; Reynolds, A. R.; Elshahawi, S. I.; Shaaban, K. A.; Ponomareva, L. V; Saunders, M. A.;  
517 Elgumati, I. S.; Zhang, Y.; Copley, G. C.; Hower, J. C.; Sunkara, M.; Morris, A. J.; Kharel, M. K.;  
518 Van Lanen, S. G.; Prendergast, M. A.; Thorson, J. S. Terfestatins B and C, New p-Terphenyl

519                   Glycosides Produced by Streptomyces Sp. RM-5–8. *Org Lett* **2015**, *17* (11), 2796–2799.  
520                   <https://doi.org/10.1021/acs.orglett.5b01203>.

521                   (40) Wu, C.; Du, C.; Gubbens, J.; Choi, Y. H.; Van Wezel, G. P. Metabolomics-Driven Discovery of a  
522                   Prenylated Isatin Antibiotic Produced by Streptomyces Species MBT28. *J Nat Prod* **2015**, *78*  
523                   (10). <https://doi.org/10.1021/acs.jnatprod.5b00276>.

524                   (41) Shaaban, M.; Shaaban, K. A.; Kelter, G.; Fiebig, H. H.; Laatsch, H. Mansouramycins E–G,  
525                   Cytotoxic Isoquinolinequinones from Marine Streptomycetes. *Mar Drugs* **2021**, *19* (12), 715.  
526                   [https://doi.org/10.3390/MD19120715/S1](https://doi.org/10.3390/MD19120715).

527                   (42) MacNeil, D. J.; Gewain, K. M.; Ruby, C. L.; Dezeny, G.; Gibbons, P. H.; MacNeil, T. Analysis of  
528                   Streptomyces Avermitilis Genes Required for Avermectin Biosynthesis Utilizing a Novel  
529                   Integration Vector. *Gene* **1992**, *111* (1), 61–68. [https://doi.org/10.1016/0378-1119\(92\)90603-M](https://doi.org/10.1016/0378-1119(92)90603-M).

531                   (43) Paget, M. S. B.; Chamberlin, L.; Atrih, A.; Foster, S. J.; Buttner, M. J. Evidence That the  
532                   Extracytoplasmic Function Sigma Factor  $\sigma(E)$  Is Required for Normal Cell Wall Structure in  
533                   Streptomyces Coelicolor A3(2). *J Bacteriol* **1999**, *181* (1), 204–211.  
534                   <https://doi.org/10.1128/jb.181.1.204-211.1999>.

535                   (44) Jiang, X.; Radko, Y.; Gren, T.; Palazzotto, E.; Jørgensen, T. S.; Cheng, T.; Xian, M.; Weber, T.;  
536                   Lee, S. Y. Distribution of  $\epsilon$ -Poly-L-Lysine Synthetases in Coryneform Bacteria Isolated from  
537                   Cheese and Human Skin. *Appl Environ Microbiol* **2021**, *87* (10), 1–8.  
538                   [https://doi.org/10.1128/AEM.01841-20/SUPPL\\_FILE/AEM.01841-20-S0003.XLSX](https://doi.org/10.1128/AEM.01841-20/SUPPL_FILE/AEM.01841-20-S0003.XLSX).

539                   (45) Mandel, M.; Higa, A. Calcium-Dependent Bacteriophage DNA Infection. *J Mol Biol* **1970**, *53*  
540                   (1), 159–162. [https://doi.org/10.1016/0022-2836\(70\)90051-3](https://doi.org/10.1016/0022-2836(70)90051-3).

541                   (46) Hanahan, D. Studies on Transformation of Escherichia Coli with Plasmids. *J Mol Biol* **1983**, *166*  
542                   (4), 557–580. [https://doi.org/10.1016/S0022-2836\(83\)80284-8](https://doi.org/10.1016/S0022-2836(83)80284-8).

543                   (47) Blin, K.; Shaw, S.; Augustijn, H. E.; Reitz, Z. L.; Biermann, F.; Alanjary, M.; Fetter, A.; Terlouw,  
544                   B. R.; Metcalf, W. W.; Helfrich, E. J. N.; van Wezel, G. P.; Medema, M. H.; Weber, T.  
545                   AntiSMASH 7.0: New and Improved Predictions for Detection, Regulation, Chemical  
546                   Structures and Visualisation. *Nucleic Acids Res* **2023**, *51* (W1), W46–W50.  
547                   <https://doi.org/10.1093/nar/gkad344>.

548                   (48) Katoh, K.; Standley, D. M. MAFFT Multiple Sequence Alignment Software Version 7:  
549                   Improvements in Performance and Usability. *Mol Biol Evol* **2013**, *30* (4), 772–780.  
550                   <https://doi.org/10.1093/molbev/mst010>.

551                   (49) Price, M. N.; Dehal, P. S.; Arkin, A. P. FastTree 2 – Approximately Maximum-Likelihood Trees  
552                   for Large Alignments. *PLoS One* **2010**, *5* (3), e9490-.

553                   (50) Letunic, I.; Bork, P. Interactive Tree Of Life (iTOL) v5: An Online Tool for Phylogenetic Tree  
554                   Display and Annotation. *Nucleic Acids Res* **2021**, *49* (W1), W293–W296.  
555                   <https://doi.org/10.1093/nar/gkab301>.

556                   (51) Blin, K.; Shaw, S.; Medema, M. H.; Weber, T. The AntiSMASH Database Version 4: Additional  
557                   Genomes and BGCs, New Sequence-Based Searches and More. *Nucleic Acids Res* **2023**,  
558                   gkad984. <https://doi.org/10.1093/nar/gkad984>.

559 (52) Lima, T. S.; Iglesias-Gato, D.; Souza, L. D. O.; Stenvang, J.; Lima, D. S.; Røder, M. A.; Brasso, K.;  
560 Moreira, J. M. A. Molecular Profiling of Docetaxel-Resistant Prostate Cancer Cells Identifies  
561 Multiple Mechanisms of Therapeutic Resistance. *Cancers* 2021, Vol. 13, Page 1290 **2021**, 13  
562 (6), 1290. <https://doi.org/10.3390/CANCERS13061290>.

563